Saturating the Maximum Success Probability Bound for Noiseless Linear Amplification Using Linear Optics

Joshua J. Guanzon,[1,*] Matthew S. Winnel,[1] Deepesh Singh,[1] Austin P. Lund,[1,2] and Timothy C. Ralph[1]

[1] *Centre for Quantum Computation and Communication Technology, School of Mathematics and Physics, The University of Queensland, St Lucia, Queensland 4072, Australia*

[2] *Dahlem Center for Complex Quantum Systems, Freie Universität Berlin, 14195 Berlin, Germany*

(Received 27 October 2023; accepted 24 April 2024; published 13 June 2024)

A noiseless linear amplifier (NLA) performs the highest-quality amplification allowable under the rules of quantum physics. Unfortunately, these same rules conspire against us via the no-cloning theorem, which constrains NLA operations to the domain of probabilistic processes. Nevertheless, they are useful for a wide variety of quantum protocols, with numerous proposals assuming access to an optimal NLA device that performs with the maximum possible success probability. Here we propose the first linear-optics NLA protocol that asymptotically achieves this success probability bound by modifying the Knill-Laflamme-Milburn near-deterministic teleporter into an amplifier.

DOI: 10.1103/PRXQuantum.5.020359

I. INTRODUCTION

A general definition for an amplifier is a device that increases the amplitude of a signal. The most-well-known types are electronic amplifiers, which act on current or voltage; through transistors, they played an important central role in the recent digital technology revolution. The more recent types are quantum amplifiers, which act on quantum states; it remains to be seen whether they will play a similar role in the upcoming quantum technology revolution. In this respect, it is important to properly investigate what is physically achievable with quantum amplifiers.

In this paper we consider quantum amplifiers that perform the best quality amplification. To understand the properties that such amplifiers would satisfy, consider a scenario where we want to amplify a coherent state $|\alpha\rangle$, with α the complex amplitude. Recall that coherent states have minimum noise profiles according to the uncertainty principle. A noiseless amplifier with gain $g \in (0, \infty)$ should produce another coherent state $|g\alpha\rangle$ since it introduces no extra noise. Furthermore, a noiseless linear amplifier (NLA) can do this without any prior knowledge of α; in other words, it acts like the operator $g^{a^\dagger a}$, since $g^{a^\dagger a}|\alpha\rangle \propto |g\alpha\rangle$.

This NLA operation is so powerful that construction of a deterministic NLA is understood to be impossible [2]. However, it is possible to make probabilistic NLAs [3], with a success probability bound $\mathbb{P}_b$ shown by the dashed black lines in Fig. 1(a). Intuitively, this is because using $|g\alpha\rangle$ with $g \geq 1$ and a balanced beam splitter, one can produce up to g^2 clones of an unknown $|\alpha\rangle$ [4], as shown for $g = \sqrt{2}$ in the inset in Fig. 1(a). Therefore, to ensure that the no-cloning theorem [5,6] is not violated, we require that no extra clones are produced on average, $g^2\mathbb{P}_b = 1$; this gives us the no-cloning bound $\mathbb{P}_b(g \geq 1) = g^{-2}$ [7]. One can apply the reverse logic and the no-deleting theorem [8] to produce the bound $\mathbb{P}_b(g \leq 1) = g^2$ for deamplification. Note that there are more formal methods for deriving this bound, such as via quantum state discrimination [9].

Despite NLAs being nondeterministic, the unrivaled quality of noiseless amplification means they are often the only path forward for many quantum protocols. This includes for applications in quantum communication [10–23], quantum repeater networks [24–32], quantum entanglement distillation [33–37], quantum improved sensing [38–42], and quantum error correction [43–46]. These protocols either presuppose the use of or can be enhanced by a maximally efficient NLA with a success probability equivalent to the bound. However, it is not apparent how to implement such an efficient NLA in optics, the natural platform for many of these schemes, without strong nonlinear interactions. It was shown in

*Corresponding author: joshua.guanzon@uq.net.au

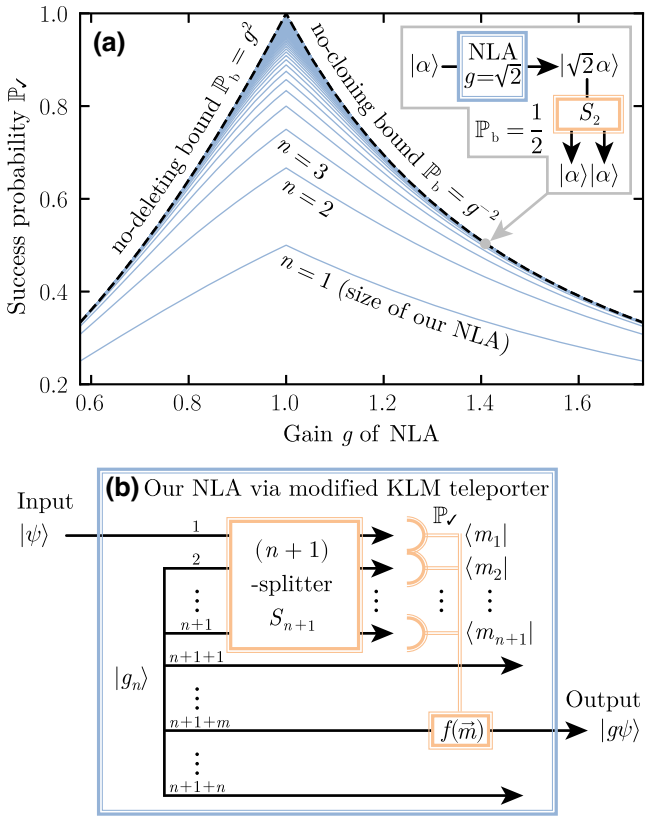

FIG. 1. The best quality quantum amplifiers (i.e., NLAs) must be probabilistic. They are bounded in probability $\mathbb{P}_b(g)$ by the dashed black lines in (a), which depends on the amount of amplification (deamplification) gain g. This prevents the violation of the no-cloning (no-deleting) theorem on average. The inset explains this for $\mathbb{P}_b(g=\sqrt{2}) = 1/2$, as this NLA could be used to produce two $|\alpha\rangle$ coherent state clones via a balanced beam splitter S_2. (b) The first linear optical NLA device, with a size parameter n, whose success probability $\mathbb{P}_\checkmark$ can saturate the bound. The input can be any arbitrary single-photon qubit state $|\psi\rangle = c_0|0\rangle + c_1|1\rangle$. Our proposal is the Knill-Laflamme-Milburn near-deterministic teleporter [1], but with the resource state $|g_n\rangle$ (consisting of n single photons entangled among $2n$ modes) being weighted to also amplify the output $|g\psi\rangle = c_0|0\rangle + gc_1|1\rangle$ with gain g. The symmetrical $(n+1)$-splitter means nearly all measurements $\langle\vec{m}| \equiv \langle m_1|\langle m_2|\cdots\langle m_{n+1}|$ at the photon number–resolving detectors are successful outcomes, except when the total photon number $m = \sum_{i=1}^{n+1} m_i$ measured is 0 or $n+1$. We plot $\mathbb{P}_\checkmark$ for sequentially increasing protocol sizes n as solid blue lines in (a), for the input state $|\psi\rangle$ that minimizes success probability.

Ref. [7] that a maximally efficient NLA could be constructed if we could somehow cause the input light to nondestructively interact with a qubit system, which requires large experimental overheads. It was also claimed in Ref. [7] that for all known linear optical NLAs the success probability is only $(1+g^2)^{-1}$. We will prove that linear optical interactions can achieve the success probability bound.

There are various methods that can perform the NLA operation [47–58], with suboptimal success probability. In particular, there has been a recent resurgence of research on NLAs [59–65] that work via quantum teleportation [66], which are called "teleamplifiers." We highlight this type of NLA because if we want a teleamplifier that can saturate the probability bound, then clearly it should also be able to act like a deterministic teleporter since $\mathbb{P}_b(g=1) = 1$. Fortunately, there already exists a deterministic teleporter as part of the well-known Knill-Laflamme-Milburn (KLM) linear optical quantum computing protocol [1]. This inspired the simple idea behind this work: modify the KLM teleporter to operate as a teleamplifier, and then verify that it is the first linear optical NLA proposal that can actually saturate the maximum probability bound $\mathbb{P}_b$ for all g.

We begin in Sec. II, where we describe our scalable teleamplifier and prove that it operates as a NLA. We then calculate the success probability of our teleamplifier in Sec. III, and we show that it asymptotically saturates the probability bound. In Sec. IV, we investigate the experimental resource requirements of our protocol at the smallest sizes. We describe how to extend the results to multiphoton input states in Sec. V. Finally, we conclude this work in Sec. VI.

II. OUR NOISELESS LINEAR AMPLIFIER

Suppose we start with an unknown quantum input state $|\psi\rangle$ containing up to a single photon (i.e., a single-rail qubit). Then a NLA operation $g^{a^\dagger a}$ should result in the following output:

$$|\psi\rangle = c_0|0\rangle + c_1|1\rangle \to |g\psi\rangle = c_0|0\rangle + gc_1|1\rangle, \qquad (1)$$

where $g \in (0,\infty)$ is the amount of gain. We propose a scalable linear optical NLA protocol, with a size parameter $n \in \mathbb{N}$, as shown in Fig. 1(b). We later show it can saturate the maximum success probability bound at asymptotically large sizes $n \to \infty$. However, we first verify that our device actually performs the claimed NLA operation in Eq. (1) and produces the correct amplified output state.

Our protocol requires the following resource state of n single photons entangled over $2n$ modes:

$$|g_n\rangle = \frac{1}{\sqrt{\mathcal{N}}}\sum_{j=0}^{n} g^{n-j}\,|1\rangle^j\,|0\rangle^{n-j}\,|0\rangle^j\,|1\rangle^{n-j}, \qquad (2)$$

with a normalization factor $\mathcal{N} = \sum_{j=0}^{n} g^{2j}$. We use the notation $|s\rangle^k = \otimes_{j=1}^{k}|s\rangle$ to mean that there are k modes each occupied by s photons. For $g=1$, this $|g_n\rangle$ state reduces to the entangled resource state used in the KLM near-deterministic teleporter [1]. We also require an $(n+$

1)-splitter S_{n+1} with scattering matrix

$$(\widetilde{S}_{n+1})_{j,k} \equiv \frac{\omega_{n+1}^{(j-1)(k-1)}}{\sqrt{n+1}}, \quad \omega_{n+1} \equiv e^{-i2\pi/(n+1)}, \tag{3}$$

whose phase ω_{n+1} configuration follows the quantum Fourier transformation. This operation scatters photons linearly as $(a_1^\dagger,\ldots,a_{n+1}^\dagger)^T \to \widetilde{S}_{n+1}(a_1^\dagger,\ldots,a_{n+1}^\dagger)^T$. Hence, this $(n+1)$-splitter could be thought of as an $(n+1)$-mode generalization of a balanced beam splitter.

As shown in Fig. 1(b), the first step of our protocol is to mix the unknown input and the first n modes of the resource state on the $(n+1)$-splitter as

$$S_{n+1}|\psi\rangle|g_n\rangle = \sum_{j=0}^{n} \frac{g^{n-j}}{\sqrt{\mathcal{N}}}[c_0 S_{n+1}|0\rangle|1\rangle^j|0\rangle^{n-j} + c_1 S_{n+1}|1\rangle|1\rangle^j|0\rangle^{n-j}]|0\rangle^j|1\rangle^{n-j}. \tag{4}$$

There are $2(n+1)$ terms in this summation, but recall we ultimately want just a pair of terms (i.e., two terms) of the form $c_0|0\rangle + gc_1|1\rangle$. We select particular terms by performing measurements that give us the total number of photons m that exit the $(n+1)$-splitter. Notice that the c_0 terms $S_{n+1}|0\rangle|1\rangle^j|0\rangle^{n-j}$ have $m=j$ photons, while the c_1 terms $S_{n+1}|1\rangle|1\rangle^j|0\rangle^{n-j}$ have $m=j+1$ photons, where $j\in\{0,\ldots,n\}$. Therefore, the outcome of $m\in\{1,\ldots,n\}$ photons exiting the $(n+1)$-splitter is associated with a pair of terms in Eq. (4). There is also a single $(c_0, j=0)$ term with $m=0$ photons and a single $(c_1, j=n)$ term with $m=n+1$ photons; measuring these m values will produce a single state output that is an error. We now verify that the rest of the m values give the correct amplified output state.

We perform photon number measurements $\langle\vec{m}| \equiv \langle m_1|\langle m_2|\cdots\langle m_{n+1}|$ immediately after the $(n+1)$-splitter, in which we measured $m=\sum_{i=1}^{n+1} m_i$ total photons. From our previous discussion, it is clear that this outcome must be due to either the $(c_0, j=m)$ term or the $(c_1, j=m-1)$ term, as all other terms do not have the correct number of photons. These two terms have nonzero probability amplitudes and, as discussed in the supplementary information for Ref. [1], due to the symmetry of S_{n+1} they are related as follows:

$$\langle\vec{m}|S_{n+1}|1\rangle^m|0\rangle^{n-m+1} \equiv p, \tag{5}$$

$$\langle\vec{m}|S_{n+1}|0\rangle|1\rangle^m|0\rangle^{n-m} = \omega_{n+1}^{f(\vec{m})}p, \tag{6}$$

which we formally prove in Appendix A. In other words, these probability amplitudes differ only by a correctable phase that depends on the known measurement outcome $f(\vec{m}) = \sum_{k=1}^{n+1}(k-1)m_k$. Using these results and Eq. (4), we find the output state will be

$$\begin{aligned}\langle\vec{m}|S_{n+1}|\psi\rangle|g_n\rangle &= \frac{g^{n-m}}{\sqrt{\mathcal{N}}}c_0\omega_{n+1}^{f(\vec{m})}p|0\rangle^m|1\rangle^{n-m} + \frac{g^{n-m+1}}{\sqrt{\mathcal{N}}}c_1 p|0\rangle^{m-1}|1\rangle^{n-m+1}\\ &= \frac{g^{n-m}p}{\sqrt{\mathcal{N}}}|0\rangle^{m-1}[\omega_{n+1}^{f(\vec{m})}c_0|0\rangle + gc_1|1\rangle]|1\rangle^{n-m}.\end{aligned} \tag{7}$$

Finally, by applying a simple phase correction $\omega_{n+1}^{f(\vec{m})a_m^\dagger a_m}$ to the mth output mode, we get the final output state

$$\begin{aligned}&\omega_{n+1}^{f(\vec{m})a_m^\dagger a_m}\langle\vec{m}|S_{n+1}|\psi\rangle|g_n\rangle\\ &= \frac{\omega_{n+1}^{f(\vec{m})}g^{n-m}p}{\sqrt{\mathcal{N}}}|0\rangle^{m-1}[c_0|0\rangle + gc_1|1\rangle]|1\rangle^{n-m}.\end{aligned} \tag{8}$$

Thus, we have verified that on the mth output mode we get the required NLA output state $|g\psi\rangle = c_0|0\rangle + gc_1|1\rangle$ for any $\langle\vec{m}|$ given we measured $m\in\{1,\ldots,n\}$ total photons. By tracing over all output modes but the mth mode and renormalizing Eq. (8), we obtain $|g\psi\rangle$ as expected.

III. SUCCESS PROBABILITY ANALYSIS

We now determine the success probability for this NLA protocol $\mathbb{P}_{\checkmark}$. We could calculate this by using the output state given in Eq. (8) and summing over all relevant success measurements $\{\forall\vec{m}|m\in\{1,\ldots,n\}\}$. However, it is easier to infer the success probability $\mathbb{P}_{\checkmark} = 1-\mathbb{P}_{\times}$ from the failure probability, since there are just two failure cases $\mathbb{P}_{\times} = \mathbb{P}_{m=0} + \mathbb{P}_{m=n+1}$. Recall that the $m=0$ case with $\langle\vec{m}| = \langle 0|^{n+1}$ has nonzero overlap only with the isolated $(c_0, j=0)$ term in Eq. (4), which gives the output

$$\langle 0|^{n+1}S_{n+1}|\psi\rangle|g_n\rangle = \frac{g^n c_0}{\sqrt{\mathcal{N}}}|1\rangle^n. \tag{9}$$

Thus, the probability of measuring $m=0$ is given by

$$\mathbb{P}_{m=0} = |\langle 0|^{n+1}S_{n+1}|\psi\rangle|g_n\rangle|^2 = \frac{g^{2n}|c_0|^2}{\mathcal{N}}. \tag{10}$$

Likewise, the $m=n+1$ case with $\langle\vec{m}_{n+1}|$ where $\vec{m}_{n+1}\in\{\forall\vec{m}|m=n+1\}$ has nonzero overlap with the isolated $(c_1, j=n)$ term in Eq. (4), which gives the output

$$\langle\vec{m}_{n+1}|S_{n+1}|\psi\rangle|g_n\rangle = \frac{c_1}{\sqrt{\mathcal{N}}}\langle\vec{m}_{n+1}|S_{n+1}|1\rangle^{n+1}|0\rangle^n. \tag{11}$$

Thus, the probability of measuring $m = n+1$ is given by

$$\begin{aligned}\mathbb{P}_{m=n+1} &= \sum_{\vec{m}|m=n+1} |\langle\vec{m}|S_{n+1}|\psi\rangle|g_n\rangle|^2 \\ &= \frac{|c_1|^2}{\mathcal{N}} \sum_{\vec{m}|m=n+1} \langle 1|^{n+1} S_{n+1}^\dagger |\vec{m}\rangle\langle\vec{m}|S_{n+1}|1\rangle^{n+1} \\ &= \frac{|c_1|^2}{\mathcal{N}}. \end{aligned} \tag{12}$$

The explanation for the third equality is that $\sum_{\vec{m}|m=n+1} |\vec{m}\rangle\langle\vec{m}|$ is the identity operator for states made from $n+1$ photons in $n+1$ modes. For example, the $n=1$ operator $\sum_{\vec{m}|m=2} |\vec{m}\rangle\langle\vec{m}| = |0\rangle|2\rangle\langle 0|\langle 2| + |1\rangle|1\rangle\langle 1|\langle 1| + |2\rangle|0\rangle\langle 2|\langle 0|$ acting on any two photons in the two-mode state $c_{02}|0\rangle|2\rangle + c_{11}|1\rangle|1\rangle + c_{20}|2\rangle|0\rangle$ will leave it unchanged. Since $S_{n+1}|1\rangle^{n+1}$ is a state with $n+1$ photons in $n+1$ modes, it will remain unchanged by the operator $\sum_{\vec{m}|m=n+1} |\vec{m}\rangle\langle\vec{m}|$.

By considering the complement of these failure outcomes, we can calculate the success probability as follows:

$$\begin{aligned}\mathbb{P}_{\checkmark} &= 1 - (\mathbb{P}_{m=0} + \mathbb{P}_{m=n+1}) \\ &= 1 - \frac{g^{2n}|c_0|^2 + |c_1|^2}{\mathcal{N}}. \end{aligned} \tag{13}$$

The closed expression for the normalization factor $\mathcal{N}$ is given by the geometric series

$$\mathcal{N} = \sum_{j=0}^{n} g^{2j} = \begin{cases} \frac{1-g^{2(n+1)}}{1-g^2}, & g \neq 1, \\ n+1, & g = 1. \end{cases} \tag{14}$$

Using this expression and the input normalization condition $|c_0|^2 + |c_1|^2 = 1$, we can get a simple closed expression for the success probability as

$$\mathbb{P}_{\checkmark} = \begin{cases} \frac{(1-g^{2n})(|c_0|^2+g^2|c_1|^2)}{1-g^{2(n+1)}}, & g \neq 1, \\ \frac{n}{n+1}, & g = 1. \end{cases} \tag{15}$$

As expected for $g = 1$, this $n/(n+1)$ expression matches the success probability for the KLM near-deterministic teleporter [1]. We plot the success probability $\mathbb{P}_{\checkmark}$ in Fig. 1(a). Since the input state (i.e., the value of c_0) chosen by the user can have any value, in the graph we therefore practice caution by assuming that we have the input state that gives the lowest success probability. From Eq. (15), the probability is proportional to $(1-g^2)|c_0|^2 + g^2$ for $g \neq 1$ with the normalization $|c_1|^2 = 1 - |c_0|^2$. If $g > 1$, then the factor $(1-g^2)$ is negative; therefore, the smallest probability is when the term $(1-g^2)|c_0|^2$ is most negative or $|c_0|^2 = 1$. The same logic can be applied in reverse for $g < 1$. In other words, the input state that minimizes the success probability is essentially a vacuum $|c_0|^2 \simeq 1$ for amplification, $g > 1$, and essentially a single photon $|c_0|^2 \simeq 0$ for deamplification, $g < 1$. Note we say "essentially" because one cannot amplify a single number state. The solid blue lines in Fig. 1(a) show that the success probability will always increase as we increase the size n of our teleamplifier. By the derivative test, one can also analytically verify that the factor $(1-g^{2n})/(1-g^{2(n+1)})$, and hence $\mathbb{P}_{\checkmark}$, always increases with n for all g.

If we consider the asymptotic limit of $n \to \infty$, we get the following expression for the factor:

$$\lim_{n\to\infty} \frac{1-g^{2n}}{1-g^{2(n+1)}} = \begin{cases} g^{-2}, & g > 1, \\ 1, & g < 1. \end{cases} \tag{16}$$

Hence, the maximum achievable success probability of our teleamplifier depends on whether we are considering amplification, $g > 1$, teleportation, $g = 1$, or deamplification, $g < 1$, as summarized below:

$$\lim_{n\to\infty} \mathbb{P}_{\checkmark} = \begin{cases} g^{-2}|c_0|^2 + |c_1|^2, & g > 1, \\ 1, & g = 1, \\ |c_0|^2 + g^2|c_1|^2, & g < 1. \end{cases} \tag{17}$$

This is a very nice expression, as we can see how the gain g affects the success probability through the different input components. At $g = 1$, we have the deterministic teleporter, and if we move away from $g = 1$, we generally have a reduction in success probability. In the amplification regime $g > 1$, this reduction acts on the $|c_0|^2$ vacuum component in the input. This makes sense, because if $|c_0|^2 \simeq 0$, then our input is essentially already completely amplified $|1\rangle$; hence, this should be deterministic. Even in the worst-case scenario with an input of $|c_0|^2 \simeq 1$, our teleamplifier's success probability saturates the no-cloning bound $\mathbb{P}_{\text{b}}(g \geq 1) = g^{-2}$. This same analysis can be applied in reverse for the deamplification regime, which shows our teleamplifier can also achieve the no-deleting bound $\mathbb{P}_{\text{b}}(g \leq 1) = g^2$.

IV. EXPERIMENTAL CONSIDERATIONS

What we demonstrated has theoretical significance; that mere linear interactions, with entanglement and measurements, are sufficient to perform amplification with the highest quality and efficiency allowed by quantum physics. We now consider the experimental requirements of our protocol in practice.

One major source of experimental complexity is the required entangled resource state $|g_n\rangle$, as defined in Eq. (2). The smallest size $|g_1\rangle$ can be made deterministically with a single photon and a beam splitter; this is equivalent to the single-photon quantum scissor NLA [3]. However, $|g_2\rangle$ cannot be made from only two single photons and a linear optical network. One suggestion [67,68] is to use a

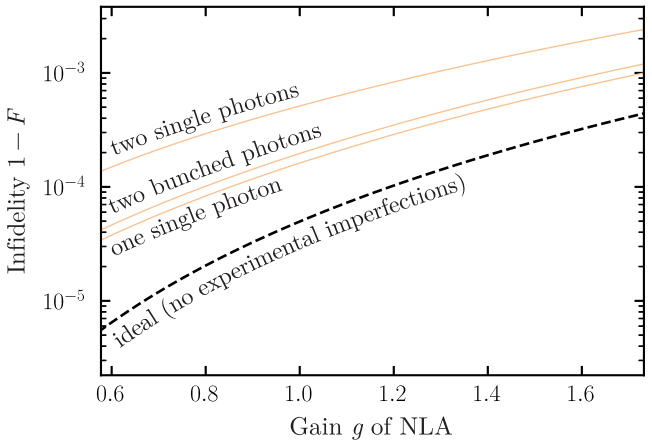

FIG. 2. Simulated performance of our NLA proposal with experimental imperfections. These imperfections are pure loss with transmissivity $\eta = 0.7$, applied independently before all detectors and on all resource modes. We amplify a coherent state $|\alpha\rangle$ with $\alpha = 0.1$, and we calculate the infidelity of the amplified output state in comparison with a perfect amplified state $|g\alpha\rangle$. The solid yellow lines are this infidelity, which depends on the type of photon number measurement $\langle\vec{m}|$. The dashed black line is the infidelity with no loss, $\eta = 1.0$.

Gaussian-boson-sampling-like device [69], which we optimized via machine learning [70] to produce $|g_2\rangle$ with very high fidelity $F > 0.999$. This is a shotgun approach with low efficiency. Instead we can draw inspiration from tailored approaches from past studies on the KLM resource state [71]. In particular, we propose a construction method like that in Ref. [72] for all $|g_n\rangle$ using $n-1$ controlled beam splitters, which can be implemented with linear-optics tools with $1/16^{n-1}$ postselection probability [71]. The details are given in Appendix B. One could factor in this resource generation probability to the overall probability of our amplifier. However, since $|g_n\rangle$ is always a known fixed state, it can be prepared off-line and stored beforehand. In this manner, our claim for achieving the probability bounds for amplifiers is analogous to the claim of Knill *et al.* [1] for achieving determinism for teleporters.

Another major consideration is experimental error. The $(\forall n, g = 1)$ edge case is the KLM teleporter, which is known to be fault tolerant from photon loss and detector inefficiencies. Furthermore, the $(n = 1, \forall g)$ edge case is the single-photon quantum scissor NLA, which has been experimentally implemented [47] and is also known to be loss tolerant [27]. Therefore, one would expect that larger n is also loss tolerant. We verify this in Fig. 2, which is from a numerical simulation of our protocol with pure loss, for small sizes $n \in \{1, 2\}$ and with a coherent state input $|\alpha\rangle$. This loss is characterized by a transmissivity η of 0.7 on all resource modes and detectors (i.e., simulating detection inefficiencies). The graph lines are of infidelity $1 - F$, where the fidelity F is the output state compared with the perfectly amplified coherent state $|g\alpha\rangle$. The dashed black line is the ideal no-loss situation, where the source of the infidelity is due to our basic protocol outputting only single-photon states. Our protocol with loss is still close to this ideal (i.e., loss tolerant), although this depends on what was measured in our protocol $\langle\vec{m}|$. The most likely outcome is detection of a single photon (which increases in probability as the gain g increases), while the second most likely outcome is detection of two bunched photons. Thus, our proposal can work well right out of the box despite inefficient detectors and lossy components. There is also the possibility of improvement by leveraging existing error correction schemes made for the KLM protocol [73].

The predominant type of error in optics is loss, which especially affects multiphoton states. This is why numerous quantum optical protocols rely on just single-photon qubit states. For example, it was shown in Ref. [27] that while a multiphoton NLA could distill a larger magnitude of entanglement through a lossy channel, a single-photon NLA has much higher entanglement rates (which takes into account success probability). Therefore, our current proposed NLA with single-photon output will be useful for achieving the highest possible entanglement rates and key rates for quantum communication purposes.

V. EXTENSION TO MULTIPHOTON STATES

There are instances where we may want to amplify unknown quantum states of light that contain multiple photons $|\phi\rangle = \sum_{j=0}^{\infty} c_j |j\rangle$. Intuitively, any physical state should be bounded in energy, where $r \gg \langle\phi|a^\dagger a|\phi\rangle$. Therefore, if we split up $|\phi\rangle$ using a large-enough r-splitter S_r as shown in Fig. 3, we can always manufacture a situation where each rail has much less than one photon on average. We can then apply our NLA to amplify each rail almost ideally. Finally, we apply the inverse r-splitter $S_r^\dagger$, which should recombine the light into a single rail $|g\phi\rangle$. This extension method was proposed in Ref. [47] using the single-photon quantum scissor NLA. We now formally verify that this physical intuition is true using our proposed NLA.

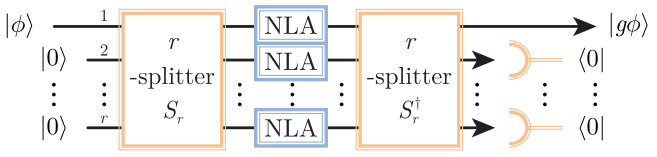

FIG. 3. Our results can be extended to unknown input states containing multiple photons $|\phi\rangle$. Intuitively, the input light is split by S_r into r rails, such that each rail has less than one photon on average. Each rail goes through our proposed NLA and is then recombined with use of $S_r^\dagger$ into a single output rail.

Instead of a superposition of number states, it is equally valid to represent any arbitrary quantum state as a superposition of coherent states $|\phi\rangle = \sum_{j=0}^{\infty} c_j |\alpha_j\rangle$. This is because coherent states $|\alpha_j\rangle$ form an overcomplete basis. However, for simplicity, for now we just calculate how a single coherent state input

$$|\alpha\rangle = e^{-|\alpha|^2/2} \sum_{j=0}^{\infty} \frac{\alpha^j}{\sqrt{j!}} |j\rangle, \tag{18}$$

is transformed by Fig. 3. One reason we moved to the coherent state basis is so we can exploit a mathematically convenient property, where a coherent state can be split into multiple dimmer coherent states, as follows:

$$S_r|\alpha\rangle|0\rangle^{r-1} = |\alpha/\sqrt{r}\rangle^r = e^{-|\alpha|^2/2} \left(\sum_{j=0}^{\infty} \frac{\alpha^j}{\sqrt{j!} r^j} |j\rangle \right)^r. \tag{19}$$

After this splitting, each rail is individually amplified by our amplifier A, where we must take into account that it can output only single-photon states as follows:

$$\begin{aligned} A^r S_r|\alpha\rangle|0\rangle^{r-1} &= \frac{e^{-|\alpha|^2/2} \left(|0\rangle + \frac{g\alpha}{\sqrt{r}}|1\rangle\right)^r}{\left(1 + \frac{|g\alpha|^2}{r}\right)^{r/2}} \\ &= \frac{e^{-|\alpha|^2/2} \prod_{j=1}^{r} \left(1 + \frac{g\alpha a_j^\dagger}{\sqrt{r}}\right) |0\rangle^r}{\left(1 + \frac{|g\alpha|^2}{r}\right)^{r/2}}, \end{aligned} \tag{20}$$

where the denominator is the normalization factor. For now, we have assumed that all NLAs A succeeded, and we will remember to account for this in the overall success probability. Next, we apply the r-splitter $S_r^\dagger$ to recombine all the rails. Recall from Eq. (3) that an r-splitter scatters photons linearly as $a_j^\dagger \to (a_1^\dagger + \cdots + \omega_r^x a_r^\dagger)/\sqrt{r}$. However, we are postselecting $\langle 0|^{r-1}$ on all rails except for the first rail; therefore, only the vacuum and $a_1^\dagger$ terms remain relevant. In other words,

$$\langle 0|^{r-1} S_r^\dagger A^r S_r|\alpha\rangle|0\rangle^{r-1} = \frac{e^{-|\alpha|^2/2} \left(1 + \frac{g\alpha a_1^\dagger}{r}\right)^r |0\rangle}{\left(1 + \frac{|g\alpha|^2}{r}\right)^{r/2}} \tag{21}$$

is our final output state for this extension protocol.

We now consider what this output state means physically. If we take the asymptotic limit in large numbers r of splitting rails, our output state is

$$\begin{aligned} \lim_{r\to\infty} \langle 0|^{r-1} S_r^\dagger A^r S_r|\alpha\rangle|0\rangle^{r-1} &= e^{-(1+g^2)|\alpha|^2/2} e^{g\alpha a_1^\dagger}|0\rangle \\ &= e^{-(1+g^2)|\alpha|^2/2} \sum_{j=0}^{\infty} \frac{(g\alpha)^j}{\sqrt{j!}} |j\rangle \\ &= e^{-|\alpha|^2/2} |g\alpha\rangle. \end{aligned} \tag{22}$$

As expected, we can see that the output is an amplified version of the input coherent state. There is a factor $e^{-|\alpha|^2/2}$ due to our postselection on zeroes. Any quantum state can be represented as a continuous superposition of coherent states on a circle in phase space since they form a complete basis [74]. In this regard, consider amplifying a superposition of N coherent states that lie equidistant on a circle:

$$|\phi\rangle = \sum_{j=1}^{N} c_j |\omega_N^j \alpha\rangle, \quad \omega_N \equiv e^{-i2\pi/N}. \tag{23}$$

With Eq. (22), our extended amplifier will output

$$\begin{aligned} \lim_{r\to\infty} \langle 0|^{r-1} S_r^\dagger A^r S_r|\phi\rangle|0\rangle^{r-1} &= \sum_{j=1}^{N} c_j e^{-|\omega_N^j \alpha|^2/2} |\omega_N^j g\alpha\rangle \\ &= e^{-|\alpha|^2/2} \sum_{j=1}^{N} c_j |\omega_N^j g\alpha\rangle \\ &= e^{-|\alpha|^2/2} |g\phi\rangle. \end{aligned} \tag{24}$$

This holds for an infinite sum of these coherent states, which form a complete basis [74]. Thus, we showed that any arbitrary multiphoton state $|\phi\rangle$ can be amplified using Fig. 3, which applies the ideal NLA transformation $g^{a^\dagger a}|\phi\rangle \propto |g\phi\rangle$ for asymptotic r rails.

We show in Appendix C that for finite r rails, this extension only approximately performs $g^{a^\dagger a}$ on the multiphoton terms. This is because the output $|g\phi\rangle = N \sum_{j=0}^{r} d_j g^j c_j |j\rangle$ has distortions d_j; however, they are negligible (i.e., $d_j \approx 1$ for small j) if r is large enough. We also show in Appendix C the success probability of this extension protocol is $\lim_{n\to\infty} \mathbb{P}_{\checkmark}^r = g^{-2r}$ for $g \geq 1$. This beats the $(1 + g^2)^{-r}$ success probability for other linear optical designs [7]. Note there is a recently discovered method for teleamplifying multiphoton states with perfect fidelity (i.e., without these distortions $d_j = 1$ for all j) in Ref. [60]; however, this is not done at the multiphoton success probability bound $\mathbb{P}_{\mathrm{b},r} = g^{-2r}$ [7]. We leave as an open question whether it is possible to combine the method in Ref. [60] with our current proposal to construct a maximally efficient, perfect-fidelity multiphoton NLA.

VI. CONCLUSION

We have presented a scalable method for constructing a quantum amplifier that performs the best quality amplification, using only linear optical tools. We verified that it is the first amplifier of its kind that saturates the quantum-limited bounds of success probability. There are numerous quantum optics protocols that assume access to such a maximally efficient amplifier. Therefore, our proposal provides a clear method to do this purely in optics, without the experimental difficulties of switching platforms or strong nonlinearities. Instead, our method relies on an entangled resource state, which we showed can be prepared beforehand with high fidelity and also with use of just linear optical tools. Finally, we demonstrated how we can extend our proposed method to allow multiphoton inputs, with much greater success probabilities than any other linear optical amplifier.

It is easy to conceive situations where the input quantum signal is very important or costly, and we want to do all we can to maximize our chances of correctly amplifying it. This is especially the case if we are considering using amplifiers in each node of a large quantum network (i.e., the quantum internet), whose success probabilities will multiply together. In these situations, it is likely that the benefits of our proposal outweigh the experimental costs of implementing it. These costs have been rapidly decreasing of late due to large investments in quantum optical protocols, which has resulted in improvements in integrated linear optical circuits, photon detectors, and generating photonic entangled cluster states.

More broadly, this research reveals that experimentally challenging nonlinear optical effects can be unnecessary. Instead, linear optical effects, with entanglement and photon detections, are sufficient to perform useful operations even at the maximum limits allowed by quantum physics. In this regard, it is fitting that a tool from the KLM scheme, the first linear optical universal quantum computing protocol, provided the necessary scaffolding to reveal this for quantum amplification.

ACKNOWLEDGMENTS

This research was supported by the Australian Research Council Centre of Excellence for Quantum Computation and Communication Technology (Project No. CE170100012).

APPENDIX A: AMPLITUDE USING PERMANENTS PROOF

In this appendix, we prove the following relations:

$$\langle\vec{m}|S_{n+1}|1\rangle^m|0\rangle^{n-m+1} \equiv p, \tag{A1}$$

$$\langle\vec{m}|S_{n+1}|0\rangle|1\rangle^m|0\rangle^{n-m} = \omega_{n+1}^{\sum_{k=1}^{n+1}(k-1)m_k} p. \tag{A2}$$

In other words, we want to verify that these two probability amplitudes are related by just a correctable phase shift, for any given photon number measurement outcome $\langle\vec{m}| \equiv \langle m_1|\langle m_2|\cdots\langle m_{n+1}|$ with $\sum_{i=1}^{n+1} m_i = m$ total photons. As an aside, we also show that the probability amplitude is given by

$$p = \frac{\mathrm{Per}(\Omega_{\vec{m}})}{\sqrt{\prod_{i=1}^{n+1} m_i!}}, \tag{A3}$$

where Per is the permanent matrix function, which is calculated like the determinant but without the alternating negative factor.

The $(n+1)$-splitter splits a single beam into $(n+1)$ equal beams. This operation S_{n+1} is therefore associated with the unitary matrix

$$\widetilde{S}_{n+1} = \frac{1}{\sqrt{n+1}} \overbrace{\begin{bmatrix} 1 & 1 & \cdots & 1 \\ 1 & \omega_{n+1} & \cdots & \omega_{n+1}^{n} \\ \vdots & \vdots & \ddots & \vdots \\ 1 & \omega_{n+1}^{n} & \cdots & \omega_{n+1}^{2n} \end{bmatrix}}^{n+1 \text{ columns}} \Bigg\}^{n+1 \text{ rows}}, \tag{A4}$$

which describes the scattering of photons as follows: $(a_1^\dagger,\ldots,a_{n+1}^\dagger)^T \to \widetilde{S}_{n+1}(a_1^\dagger,\ldots,a_{n+1}^\dagger)^T$. For example, injection of a single photon into the cth input port $a_c^\dagger|0\rangle^{n+1}$ is related to the cth column of $\widetilde{S}_{n+1}$, where $a_c^\dagger \to \sum_{r=1}^{n+1}(\widetilde{S}_{n+1})_{r,c}a_r^\dagger = \sum_{r=1}^{n+1}\frac{\omega_{n+1}^{(c-1)(r-1)}}{\sqrt{n+1}}a_r^\dagger$. The probability amplitude for a particular single-photon input and output combination is given by

$$\langle 0|^{n+1}a_r S_{n+1}a_c^\dagger|0\rangle^{n+1} = \frac{\omega_{n+1}^{(c-1)(r-1)}}{\sqrt{n+1}}, \tag{A5}$$

which is the (r,c) element in $\widetilde{S}_{n+1}$. For a more general multiple-photon input, the scattering probability amplitudes are related to multiple elements of $\widetilde{S}_{n+1}$. Suppose we have an arbitrary m-photon input state $|\vec{m}'\rangle \equiv \otimes_{i=1}^{n+1}|m_i'\rangle = \prod_{i=1}^{n+1}[(a_i^\dagger)^{m_i'}/\sqrt{m_i'!}]|0\rangle^{n+1}$, where $\sum_{i=1}^{n+1} m_i' = m$. Then we have the following probability amplitude:

$$\langle\vec{m}|S_{n+1}|\vec{m}'\rangle = \frac{\mathrm{Per}(\Omega_{\vec{m},\vec{m}'})}{\sqrt{\prod_{i=1}^{n+1} m_i!m_i'!}}. \tag{A6}$$

This is a well-known relation from boson sampling studies [75–77]; for example, Eq. (7) in Ref. [77]. $\Omega_{\vec{m},\vec{m}'}$ is an $m \times m$ matrix constructed by one taking the elements of $\widetilde{S}_{n+1}$ by repeating column c m_c' times and row r m_r times. This is more easily understood by considering a specific example, as outlined in the next paragraph.

Let us consider the $n = 2$ amplifier case. This requires the three-splitter S_3, associated with the following scattering unitary matrix:

$$\widetilde{S}_3 = \frac{1}{\sqrt{3}} \begin{bmatrix} 1 & 1 & 1 \\ 1 & \omega_3 & \omega_3^2 \\ 1 & \omega_3^2 & \omega_3^4 \end{bmatrix}. \tag{A7}$$

Suppose we want to calculate the probability amplitude for the input $\vec{m}' = (1, 1, 0)$ and output $\vec{m} = (0, 2, 0)$. This means we need to consider the elements of $\widetilde{S}_3$ made from the first two columns and repeating the second row twice, as follows:

$$\Omega_{(0,2,0),(1,1,0)} = \frac{1}{\sqrt{3}} \begin{bmatrix} 1 & \omega_3 \\ 1 & \omega_3 \end{bmatrix}. \tag{A8}$$

Taking the permanent of this matrix, we can now calculate the probability amplitude as

$$p' = \langle 0|\langle 2|\langle 0|S_3|1\rangle|1\rangle|0\rangle = \frac{\mathrm{Per}(\Omega_{(0,2,0),(1,1,0)})}{\sqrt{2}} \tag{A9}$$

using Eq. (A6). Similarly, for a different input $\vec{m}' = (0, 1, 1)$ but same output $\vec{m} = (0, 2, 0)$, we construct the following matrix:

$$\Omega_{(0,2,0),(0,1,1)} = \frac{1}{\sqrt{3}} \begin{bmatrix} \omega_3 & \omega_3^2 \\ \omega_3 & \omega_3^2 \end{bmatrix}, \tag{A10}$$

whose permanent is used to calculate the probability amplitude $\langle 0|\langle 2|\langle 0|S_3|0\rangle|1\rangle|1\rangle$. However, there is a property of permanents where

$$\mathrm{Per} \begin{bmatrix} au_{11} & au_{12} \\ bu_{21} & bu_{22} \end{bmatrix} = ab\mathrm{Per} \begin{bmatrix} u_{11} & u_{12} \\ u_{21} & u_{22} \end{bmatrix}, \tag{A11}$$

which we can use to connect the two permanents under investigation:

$$\begin{aligned} \mathrm{Per}(\Omega_{(0,2,0),(0,1,1)}) &= \mathrm{Per}\left(\frac{1}{\sqrt{3}} \begin{bmatrix} \omega_3 & \omega_3^2 \\ \omega_3 & \omega_3^2 \end{bmatrix} \right) \\ &= \omega_3^2 \mathrm{Per}\left(\frac{1}{\sqrt{3}} \begin{bmatrix} 1 & \omega_3 \\ 1 & \omega_3 \end{bmatrix} \right) \\ &= \omega_3^2 \mathrm{Per}(\Omega_{(0,2,0),(1,1,0)}). \end{aligned} \tag{A12}$$

Thus, we have shown that these two amplitudes are related by just a phase

$$\begin{aligned} \langle 0|\langle 2|\langle 0|S_3|0\rangle|1\rangle|1\rangle &= \omega_3^2 \langle 0|\langle 2|\langle 0|S_3|1\rangle|1\rangle|0\rangle \\ &= \omega_3^2 p', \end{aligned} \tag{A13}$$

which agrees with Eq. (A2), since $\sum_{k=1}^{n+1}(k-1)m_k = 2$ for this $\vec{m} = (0, 2, 0)$ example.

We consider generalizing this result to more modes, with inputs of the form $|1\rangle^m|0\rangle^{n-m+1}$ and $|0\rangle|1\rangle^m|0\rangle^{n-m}$, and arbitrary measurements $\langle\vec{m}|$. For the amplitude $\langle\vec{m}|S_{n+1}|1\rangle^m|0\rangle^{n-m+1}$, we require the matrix be made from the first m columns of $\widetilde{S}_{n+1}$ as follows:

$$\Omega_{\vec{m}} = \frac{1}{\sqrt{n+1}} \overbrace{\begin{bmatrix} 1 & \omega_{n+1}^{r_1} & \cdots & \omega_{n+1}^{(m-1)r_1} \\ \vdots & \vdots & \ddots & \vdots \\ 1 & \omega_{n+1}^{r_m} & \cdots & \omega_{n+1}^{(m-1)r_m} \end{bmatrix}}^{m \text{ columns}} \Bigg\} m \text{ rows}. \tag{A14}$$

Here $\vec{r} = \{r_1, \ldots, r_m\}$ is the row power contribution to the phase, associated with measurement outcomes $\vec{m} = (m_1, \ldots, m_{n+1})$. We have m_r repeats of row r, which have a row power contribution of $r - 1$. For example, for the measurement outcome $\vec{m} = (1, 2, 1)$, we have $\vec{r} = \{0, 1, 1, 2\}$. The order of the multiset $\vec{r}$ does not matter since the permanent is invariant under row permutations. By the definition of how $\vec{r}$ and $\vec{m}$ are related, we also have the useful identity

$$\sum_{j=1}^{m} r_j = \sum_{k=1}^{n+1} (k-1)m_k. \tag{A15}$$

Thus, using Eq. (A6), we have the case that

$$p \equiv \langle\vec{m}|S_{n+1}|1\rangle^m|0\rangle^{n-m+1} = \frac{\mathrm{Per}(\Omega_{\vec{m}})}{\sqrt{\prod_{i=1}^{n+1} m_i!}}. \tag{A16}$$

Similarly, for the probability amplitude $\langle\vec{m}|S_{n+1}|0\rangle|1\rangle^m|0\rangle^{n-m}$ we require the matrix be made from the second to $(m+1)$th columns of $\widetilde{S}_{n+1}$:

$$\Omega'_{\vec{m}} = \frac{1}{\sqrt{n+1}} \overbrace{\begin{bmatrix} \omega_{n+1}^{r_1} & \omega_{n+1}^{2r_1} & \cdots & \omega_{n+1}^{mr_1} \\ \vdots & \vdots & \ddots & \vdots \\ \omega_{n+1}^{r_m} & \omega_{n+1}^{2r_m} & \cdots & \omega_{n+1}^{mr_m} \end{bmatrix}}^{m \text{ columns}} \Bigg\} m \text{ rows}. \tag{A17}$$

The permanent property in Eq. (A11) holds in general for matrix U of any size, where multiplying any row or column by a scalar a changes its permanent from $\mathrm{Per}(U)$ to $a\mathrm{Per}(U)$. Thus, we can show the relationship between the

two permanents is

$$\mathrm{Per}(\Omega'_{\vec{m}}) = \mathrm{Per}\left(\frac{1}{\sqrt{n+1}}\begin{bmatrix}\omega_{n+1}^{r_1} & \omega_{n+1}^{2r_1} & \cdots & \omega_{n+1}^{mr_1}\\ \vdots & \vdots & \ddots & \vdots\\ \omega_{n+1}^{r_m} & \omega_{n+1}^{2r_m} & \cdots & \omega_{n+1}^{mr_m}\end{bmatrix}\right) = \prod_{i=1}^{m}\omega_{n+1}^{r_i}\,\mathrm{Per}\left(\frac{1}{\sqrt{n+1}}\begin{bmatrix}1 & \omega_{n+1}^{r_1} & \cdots & \omega_{n+1}^{(m-1)r_1}\\ \vdots & \vdots & \ddots & \vdots\\ 1 & \omega_{n+1}^{r_m} & \cdots & \omega_{n+1}^{(m-1)r_m}\end{bmatrix}\right)$$
$$= \omega_{n+1}^{\sum_{k=1}^{n+1}(k-1)m_k}\,\mathrm{Per}(\Omega_{\vec{m}}), \tag{A18}$$

where we used the identity in Eq. (A15) to simplify the phase factor as $\prod_{i=1}^{m}\omega_{n+1}^{r_i} = \omega_{n+1}^{\sum_{i=1}^{m} r_i} = \omega_{n+1}^{\sum_{k=1}^{n+1}(k-1)m_k}$. Hence, with use of Eq. (A6) the two amplitudes are related by a simple phase factor

$$\begin{aligned}\langle\vec{m}|S_{n+1}|0\rangle|1\rangle^m|0\rangle^{n-m} &= \frac{\mathrm{Per}(\Omega'_{\vec{m}})}{\sqrt{\prod_{i=1}^{n+1} m_i!}}\\ &= \omega_{n+1}^{\sum_{k=1}^{n+1}(k-1)m_k}\frac{\mathrm{Per}(\Omega_{\vec{m}})}{\sqrt{\prod_{i=1}^{n+1} m_i!}}\\ &= \omega_{n+1}^{\sum_{k=1}^{n+1}(k-1)m_k}\,p,\end{aligned} \tag{A19}$$

as needed to be proven.

APPENDIX B: GENERATING THE RESOURCE STATE

The main challenge for implementing our protocol is the required entangled resource state $|g_n\rangle$, as defined in Eq. (2). The smallest size $n = 1$ requires

$$|g_1\rangle = \frac{|1\rangle|0\rangle + g|0\rangle|1\rangle}{\sqrt{1+g^2}}, \tag{B1}$$

which can be generated easily enough by sticking a single photon through an unbalanced beam splitter $S_2(\tau)$ with transmissivity $\tau = g^2/(1+g^2)$. This gives us

$$S_2(\tau)|1\rangle|0\rangle = \sqrt{1-\tau}|1\rangle|0\rangle + \sqrt{\tau}|0\rangle|1\rangle = |g_1\rangle, \tag{B2}$$

which makes our $n = 1$ protocol equivalent to the single-photon quantum scissor teleampifier protocol [3]. However, the resource complexity increases for size $n = 2$, which requires the entangled state

$$|g_2\rangle = \frac{|1\rangle|1\rangle|0\rangle|0\rangle + g|1\rangle|0\rangle|0\rangle|1\rangle + g^2|0\rangle|0\rangle|1\rangle|1\rangle}{\sqrt{1+g^2+g^4}}. \tag{B3}$$

Even though each term has the same number of photons, it is not apparent how one could generate this entangled state from two single photons. We will describe two different methods for generating these states via postselection. Note that we are imagining a situation where this resource state is prepared off-line, or before the unknown input state has arrived at our amplifier.

1. Using Gaussian boson sampling

There are methods based on Gaussian boson sampling [69] that allows us to generate these $|g_n\rangle$ entangled states with high fidelity using squeezed displaced light, a linear optical network, and photon detection [67,68]. It is known that by postselecting on a particular measurement on some output modes $\langle m_1|\cdots\langle m_s|$, we can herald a wide variety of quantum states in the remaining output modes [67,68]. In particular, this procedure was used in Ref. [79] to create similar quantum states as $|g_n\rangle$, consisting of multiple single photons entangled over numerous modes.

We optimized all the parameters in Fig. 4 for fidelity with $|g_2\rangle$ with gain $g = \sqrt{2}$, and we heralded on the photon measurement $\langle 1|^5$ (hence in this case $n = 2$ and $s = 5$). We optimized all the parameters using a machine learning algorithm called "basin hopping," as described in Ref. [70]. We were able to find a configuration that makes this resource state with high fidelity $F > 0.99$, with success probability of approximately 10^{-8}. Our code that implements this algorithm is provided in Ref. [80].

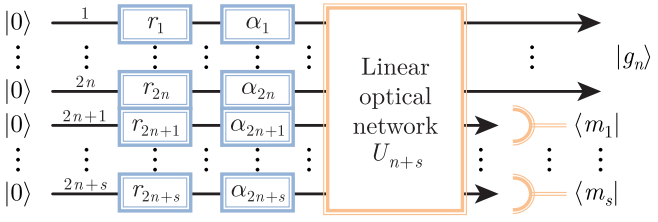

FIG. 4. We can optimize the device parameters to herald the entanglement resource state $|g_n\rangle$ with high fidelity. The first column contains squeezers with r_j squeezing parameters. The second column contains displacement operators with α_j displacement parameters. The network U_{n+s} is decomposed into beam splitters [78], whose transmission and phase parameters are also optimized. The photon detection pattern $\langle m_1|\cdots\langle m_s|$ is chosen beforehand.

2. Using controlled beam splitters

We can consider a much more tailored approach for constructing these resource states, using a similar method as Eq. (B2), where we can generate $|g_1\rangle$ using a single photon and a beam splitter. In Fig. 5, we show how to generate $|g_2\rangle$ using two single photons, a beam splitter $S_{2,4}(\tau_1)$ with transmissivity $\tau_1 = (g^2+g^4)/(1+g^2+g^4)$, and a photon number–controlled beam splitter $C_2S_{1,3}(\tau_2)$ with transmissivity $\tau_2 = g^2/(1+g^2)$. $C_2S_{1,3}(\tau_2)$ implements the beam-splitter operation only if the control mode contains zero photons, which can be done with linear optical tools with 1/16 postselection probability (since it can be done with two nonlinear sign gates with 1/4 success probability [71]). For clarity, we include mode numbers as subscripts to the operators and kets, if the modes are unordered.

We consider how one can use these controlled beam splitters to construct $|g_n\rangle$ for general sizes n. First, recognize that the resource state can be rewritten as

$$|g_n\rangle = \frac{1}{\sqrt{\mathcal{N}}}\sum_{j=0}^{n}(gP)^j|1\rangle^n|0\rangle^n, \tag{B4}$$

where P is a mode-shifting operator, which simply rotates the position of the states by one in the clockwise direction, i.e., $P|a_1\rangle|a_2\rangle\cdots|a_{2n}\rangle = |a_2\rangle\cdots|a_{2n}\rangle|a_1\rangle$. To better understand the construction method, we can rewrite the last two terms $j \in \{n-1, n\}$ of $|g_n\rangle$ as

$$\begin{aligned}
|g_{n,M=1}\rangle &= \frac{1}{\sqrt{\mathcal{N}}}\left[\sum_{j=0}^{n-2}(gP)^j|1\rangle^n|0\rangle^n + g^{n-1}|1\rangle|0\rangle^{n-1}|0\rangle|1\rangle^{n-1} + g^n|0\rangle|0\rangle^{n-1}|1\rangle|1\rangle^{n-1}\right]\\
&= \frac{1}{\sqrt{\mathcal{N}}}\left[\sum_{j=0}^{n-2}(gP)^j|1\rangle^n|0\rangle^n + g^{n-1}|0\rangle_{2,\ldots,n}^{n-1}|1\rangle_{n+2,..,2n}^{n-1}(|1\rangle|0\rangle + g|0\rangle|1\rangle)_{1,n+1}\right]\\
&= \frac{C_2S_{1,n+1}\left(\frac{g^2}{1+g^2}\right)}{\sqrt{\mathcal{N}}}\left[\sum_{j=0}^{n-2}(gP)^j|1\rangle^n|0\rangle^n + g^{n-1}\sqrt{1+g^2}|0\rangle_{2,\ldots,n}^{n-1}|1\rangle_{n+2,..,2n}^{n-1}|1\rangle_1|0\rangle_{n+1}\right]\\
&= \frac{C_2S_{1,n+1}\left(\frac{g^2}{1+g^2}\right)}{\sqrt{\mathcal{N}}}\left[\sum_{j=0}^{n-2}(gP)^j|1\rangle^n|0\rangle^n + g^{n-1}\sqrt{1+g^2}|1\rangle|0\rangle^n|1\rangle^{n-1}\right].
\end{aligned} \tag{B5}$$

We can repeat this process multiple times by contracting this remainder term with the next last j term. Hence, after using photon number–controlled beam splitters M times, we can rewrite $|g_n\rangle$ as

$$|g_{n,M}\rangle = \frac{\prod_{i=2}^{M+1}C_iS_{i-1,n+i-1}\left(\frac{\sum_{k=1}^{i-1}g^{2k}}{\sum_{k=0}^{i-1}g^{2k}}\right)}{\sqrt{\mathcal{N}}}\left[\sum_{j=0}^{n-M-1}(gP)^j|1\rangle^n|0\rangle^n + g^{n-M}\sqrt{\sum_{l=0}^{M}g^{2l}}|1\rangle^M|0\rangle^n|1\rangle^{n-M}\right], \tag{B6}$$

$$\begin{aligned}
|g_{n,M=n-1}\rangle &= \frac{\prod_{i=2}^{n}C_iS_{i-1,n+i-1}\left(\frac{\sum_{k=1}^{i-1}g^{2k}}{\sum_{k=0}^{i-1}g^{2k}}\right)}{\sqrt{\mathcal{N}}}\left[|1\rangle^n|0\rangle^n + g\sqrt{\sum_{l=0}^{n-1}g^{2l}}|1\rangle^{n-1}|0\rangle^n|1\rangle\right]\\
&= \prod_{i=2}^{n}C_iS_{i-1,n+i-1}\left(\frac{\sum_{k=1}^{i-1}g^{2k}}{\sum_{k=0}^{i-1}g^{2k}}\right)S_{n,2n}\left(\frac{\sum_{k=1}^{n}g^{2k}}{\sum_{k=0}^{n}g^{2k}}\right)|1\rangle^n|0\rangle^n.
\end{aligned} \tag{B7}$$

Note we have assumed that the normalization factor is given by $\mathcal{N} = \sum_{j=0}^{n}g^{2j}$. This representation of $|g_n\rangle$ shows how one can construct it using n single photons, one beam splitter, and $n-1$ photon number–controlled beam splitters. Hence, we have shown that we can in theory construct the required resource states exactly with linear optical tools, with a success probability of $1/16^{n-1}$ [71]. Our proposed method is quite similar to the method in Ref.

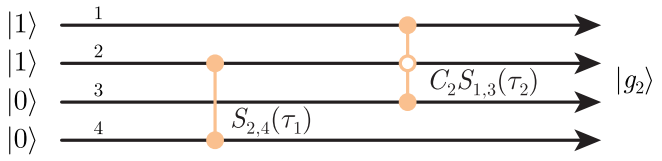

FIG. 5. Protocol for the generation of the resource state $|g_2\rangle$ using two single photons $|1\rangle|1\rangle|0\rangle|0\rangle$, a beam splitter $S_{2,4}(\tau_1)$, and a photon number–controlled beam splitter $C_2S_{1,3}(\tau_2)$. The vertical bar with solid dots represents a beam splitter between those modes. The empty dot represents the control mode that implements a beam splitter between the solid dots if it has zero photons.

[72]; however, the proposal in in Ref. [72] generates two copies of $|g_n\rangle$ using $2(n-1)$ controlled gates.

APPENDIX C: FINITE EXTENSION TO MULTIPHOTON STATES

As explained in Sec. V, we can use r copies of our single-photon protocol A as per Fig. 3 to get multiphoton outputs. For a coherent state input $|\alpha\rangle$, we get the output given in Eq. (21). We can rewrite this output state as

$$\begin{aligned}|\widetilde{g\alpha}_r\rangle &= \langle 0|^{r-1} S_r^\dagger A^r S_r |\alpha\rangle|0\rangle^{r-1} \\ &= \frac{e^{-|\alpha|^2/2}\left(1+\frac{g\alpha a_1^\dagger}{r}\right)^r|0\rangle}{\left(1+\frac{|g\alpha|^2}{r}\right)^{r/2}} \\ &= \frac{e^{-|\alpha|^2/2}\sum_{j=0}^r \binom{r}{j}\left(\frac{g\alpha}{r}\right)^j\sqrt{j!}|j\rangle}{\left(1+\frac{|g\alpha|^2}{r}\right)^{r/2}},\end{aligned} \tag{C1}$$

where we used the binomial theorem. The normalized form of this output state is given by

$$\begin{aligned}|\widetilde{g\alpha}'_r\rangle &= \frac{\sum_{j=0}^r \binom{r}{j}\left(\frac{g\alpha}{r}\right)^j\sqrt{j!}|j\rangle}{\sqrt{\sum_{k=0}^r \binom{r}{k}^2\left(\frac{g\alpha}{r}\right)^{2k}k!}} \\ &= e^{-|g\alpha|^2/2}\sum_{j=0}^r d_j\frac{(g\alpha)^j}{\sqrt{j!}}|j\rangle,\end{aligned} \tag{C2}$$

$$d_j = \frac{e^{|g\alpha|^2/2}\binom{r}{j}j!}{r^j\sqrt{\sum_{k=0}^r \binom{r}{k}^2\left(\frac{g\alpha}{r}\right)^{2k}k!}}. \tag{C3}$$

We have written this state in a form close to a coherent state, except for a distortion factor d_j applied to the jth photon number coefficient and an r photon cutoff.

A comparison between Eq. (C2) and the asymptotic case given by normalized Eq. (21) suggests that $\lim_{r\to\infty} d_j = 1$ for all j. We plot these distortion values d_j in Fig. 6 as a function of extension protocol size r. We can see that indeed these distortion factors tend toward a negligible effect $d_j \approx 1$ as r becomes large. We can also see that higher photon numbers j have larger distortions. Thus, for good fidelity in higher photon numbers, we need to split the input by more r rails, which matches our physical intuition.

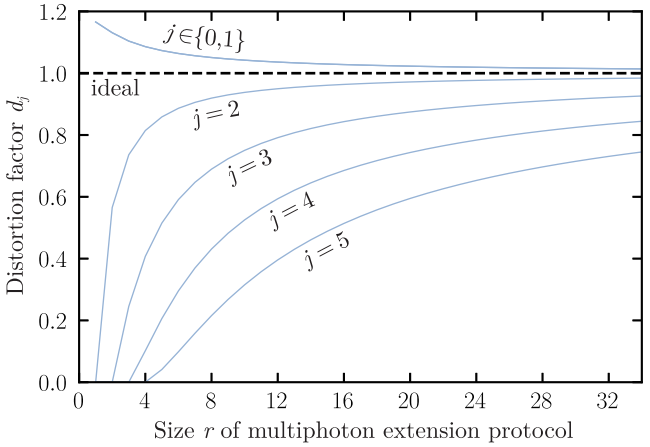

FIG. 6. Distortion factor d_j in the photon number state $|j\rangle$ coefficient of the output state $|\widetilde{g\alpha}'_r\rangle$. This state is the output from the r rails multiphoton extension protocol of our NLA device, with a given coherent state input $|\alpha\rangle$. Here we have chosen an initial amplitude α of 0.5 and with gain $g = 2$. The solid blue lines shows how the jth distortion factor, associated with the coefficient of $|j\rangle$, scales with protocol size r. Ideally, the distortion factors should be $d_j = 1$ (i.e., no distortion), as shown by the dashed black line.

We may calculate the success probability of the extension component with r rails as

$$\begin{aligned}\mathbb{P}_r &= \langle\widetilde{g\alpha}_r|\widetilde{g\alpha}_r\rangle \\ &= \frac{e^{-|\alpha|^2}\sum_{j=0}^r \binom{r}{j}^2\left(\frac{g\alpha}{r}\right)^{2j}j!}{\left(1+\frac{|g\alpha|^2}{r}\right)^r}.\end{aligned} \tag{C4}$$

We need to include the probability for the r copies of the NLA A to successfully amplify, which gives us an overall success probability of our protocol as

$$\mathbb{P}_{\checkmark,r} = \mathbb{P}_{\checkmark}^r\mathbb{P}_r. \tag{C5}$$

To understand how success probability scales with our NLAs, we consider only amplification $g > 1$ and that our NLAs A are asymptotically large, $n \to \infty$. Then we can apply Eq. (17), as follows:

$$\lim_{n\to\infty}\mathbb{P}_{\checkmark,r} = \frac{\left(g^{-2}+|\alpha|^2\right)^r e^{-|\alpha|^2}\sum_{j=0}^r \binom{r}{j}^2\left(\frac{g\alpha}{r}\right)^{2j}j!}{\left(1+\frac{|g\alpha|^2}{r}\right)^r}. \tag{C6}$$

As explained in Sec. III, the lowest success probability for amplification with our NLAs occurs for effectively vacuum input, or in this case $\alpha = 0$. This gives us a final success probability scaling of

$$\lim_{n\to\infty} \mathbb{P}_{\checkmark,r} = g^{-2r}, \tag{C7}$$

which matches the multiphoton bounds [7,9].

[1] E. Knill, R. Laflamme, and G. J. Milburn, A scheme for efficient quantum computation with linear optics, Nature **409**, 46 (2001).

[2] H. Heffner, The fundamental noise limit of linear amplifiers, Proc. IRE **50**, 1604 (1962).

[3] T. C. Ralph and A. P. Lund, in *AIP Conference Proceedings* (American Institute of Physics, Calgary, 2009), Vol. 1110, p. 155.

[4] J. Fiurášek, Optimal probabilistic cloning and purification of quantum states, Phys. Rev. A **70**, 032308 (2004).

[5] W. K. Wootters and W. H. Zurek, A single quantum cannot be cloned, Nature **299**, 802 (1982).

[6] D. Dieks, Communication by EPR devices, Phys. Lett. A **92**, 271 (1982).

[7] N. A. McMahon, A. P. Lund, and T. C. Ralph, Optimal architecture for a nondeterministic noiseless linear amplifier, Phys. Rev. A **89**, 023846 (2014).

[8] A. Kumar Pati and S. L. Braunstein, Impossibility of deleting an unknown quantum state, Nature **404**, 164 (2000).

[9] S. Pandey, Z. Jiang, J. Combes, and C. M. Caves, Quantum limits on probabilistic amplifiers, Phys. Rev. A **88**, 033852 (2013).

[10] N. Gisin, S. Pironio, and N. Sangouard, Proposal for implementing device-independent quantum key distribution based on a heralded qubit amplifier, Phys. Rev. Lett. **105**, 070501 (2010).

[11] R. Blandino, A. Leverrier, M. Barbieri, J. Etesse, P. Grangier, and R. Tualle-Brouri, Improving the maximum transmission distance of continuous-variable quantum key distribution using a noiseless amplifier, Phys. Rev. A **86**, 012327 (2012).

[12] M. Mičuda, I. Straka, M. Miková, M. Dušek, N. J. Cerf, J. Fiurášek, and M. Ježek, Noiseless loss suppression in quantum optical communication, Phys. Rev. Lett. **109**, 180503 (2012).

[13] B. Xu, C. Tang, H. Chen, W. Zhang, and F. Zhu, Improving the maximum transmission distance of four-state continuous-variable quantum key distribution by using a noiseless linear amplifier, Phys. Rev. A **87**, 062311 (2013).

[14] M. Ghalaii, C. Ottaviani, R. Kumar, S. Pirandola, and M. Razavi, Long-distance continuous-variable quantum key distribution with quantum scissors, IEEE J. Sel. Top. Quantum Electron. **26**, 1 (2020).

[15] L. Zhou, Y.-B. Sheng, and G.-L. Long, Device-independent quantum secure direct communication against collective attacks, Sci. Bull. **65**, 12 (2020).

[16] Y. Li, Y. Guo, X. Ruan, and W. Zhao, Improving the discrete-modulated continuous-variable measurement-device-independent quantum key distribution with quantum scissors, Int. J. Theor. Phys. **60**, 1949 (2021).

[17] B.-W. Xu, J. Zhang, L. Zhou, W. Zhong, and Y.-B. Sheng, Feasible noiseless linear amplification for single-photon qudit and two-photon hyperentanglement encoded in three degrees of freedom, Quantum Inf. Process. **20**, 1 (2021).

[18] E. Villaseñor and R. Malaney, in *2021 IEEE Global Communications Conference (GLOBECOM)* (IEEE, Madrid, 2021), p. 1.

[19] M. He, R. Malaney, and R. Aguinaldo, Teleportation of discrete-variable qubits via continuous-variable lossy channels, Phys. Rev. A **105**, 062407 (2022).

[20] J. Zhao, H. Jeng, L. O. Conlon, S. Tserkis, B. Shajilal, K. Liu, T. C. Ralph, S. M. Assad, and P. K. Lam, Enhancing quantum teleportation efficacy with noiseless linear amplification, Nat. Commun. **14**, 4745 (2023).

[21] M. N. Notarnicola and S. Olivares, Long-distance continuous-variable quantum key distribution with feasible physical noiseless linear amplifiers, Phys. Rev. A **108**, 022404 (2023).

[22] J. Fiurášek, Analysis of continuous-variable quantum teleportation enhanced by measurement-based noiseless quantum amplification, Opt. Express **32**, 2527 (2024).

[23] J.-Q. Gu, Y.-P. Feng, M.-M. Du, W. Zhong, Y.-B. Sheng, and L. Zhou, Efficient noiseless linear amplification protocol for single-photon state using imperfect auxiliary photon source, Laser Phys. Lett. **21**, 025203 (2024).

[24] J. Dias and T. C. Ralph, Quantum repeaters using continuous-variable teleportation, Phys. Rev. A **95**, 022312 (2017).

[25] J. Dias, M. S. Winnel, N. Hosseinidehaj, and T. C. Ralph, Quantum repeater for continuous-variable entanglement distribution, Phys. Rev. A **102**, 052425 (2020).

[26] K. P. Seshadreesan, H. Krovi, and S. Guha, Continuous-variable quantum repeater based on quantum scissors and mode multiplexing, Phys. Rev. Res. **2**, 013310 (2020).

[27] M. S. Winnel, J. J. Guanzon, N. Hosseinidehaj, and T. C. Ralph, Overcoming the repeaterless bound in continuous-variable quantum communication without quantum memories, ArXiv:2105.03586.

[28] R. Laurenza, N. Walk, J. Eisert, and S. Pirandola, Rate limits in quantum networks with lossy repeaters, Phys. Rev. Res. **4**, 023158 (2022).

[29] I. J. Tillman, A. Rubenok, S. Guha, and K. P. Seshadreesan, Supporting multiple entanglement flows through a continuous-variable quantum repeater, Phys. Rev. A **106**, 062611 (2022).

[30] J. Dias, M. S. Winnel, W. J. Munro, T. C. Ralph, and K. Nemoto, Distributing entanglement in first-generation discrete-and continuous-variable quantum repeaters, Phys. Rev. A **106**, 052604 (2022).

[31] M. Ghalaii, P. Papanastasiou, and S. Pirandola, Composable end-to-end security of Gaussian quantum networks with untrusted relays, npj Quantum Inf. **8**, 105 (2022).

[32] A. J. E. Bjerrum, J. B. Brask, J. S. Neergaard-Nielsen, and U. L. Andersen, Quantum repeater using two-mode

squeezed states and atomic noiseless amplifiers, Phys. Rev. A **107**, 042606 (2023).
[33] S. L. Zhang, S. Yang, X. B. Zou, B. S. Shi, and G. C. Guo, Protecting single-photon entangled state from photon loss with noiseless linear amplification, Phys. Rev. A **86**, 034302 (2012).
[34] K. P. Seshadreesan, H. Krovi, and S. Guha, Continuous-variable entanglement distillation over a pure loss channel with multiple quantum scissors, Phys. Rev. A **100**, 022315 (2019).
[35] Y. Liu, K. Zheng, H. Kang, D. Han, M. Wang, L. Zhang, X. Su, and K. Peng, Distillation of Gaussian Einstein-Podolsky-Rosen steering with noiseless linear amplification, npj Quantum Inf. **8**, 1 (2022).
[36] M. He and R. Malaney, Teleportation of hybrid entangled states with continuous-variable entanglement, Sci. Rep. **12**, 17169 (2022).
[37] C. Mauron and T. C. Ralph, Comparison of techniques for distillation of entanglement over a lossy channel, Phys. Rev. A **106**, 062603 (2022).
[38] M. A. Usuga, C. R. Müller, C. Wittmann, P. Marek, R. Filip, C. Marquardt, G. Leuchs, and U. L. Andersen, Noise-powered probabilistic concentration of phase information, Nat. Phys. **6**, 767 (2010).
[39] J. Zhao, J. Dias, J. Y. Haw, T. Symul, M. Bradshaw, R. Blandino, T. Ralph, S. M. Assad, and P. K. Lam, Quantum enhancement of signal-to-noise ratio with a heralded linear amplifier, Optica **4**, 1421 (2017).
[40] Y. Xia, Q. Zhuang, W. Clark, and Z. Zhang, Repeater-enhanced distributed quantum sensing based on continuous-variable multipartite entanglement, Phys. Rev. A **99**, 012328 (2019).
[41] A. Karsa, M. Ghalaii, and S. Pirandola, Noiseless linear amplification in quantum target detection using Gaussian states, Quantum Sci. Technol. **7**, 035026 (2022).
[42] J. Tang, Y. Liu, J. Li, Y. Cao, Z. Deng, H. Yu, L. Shi, and J. Wei, Improving the sensitivity of distributed phase estimation under noisy Gaussian environment with noiseless linear amplification, Mod. Phys. Lett. B **37**, 2350170 (2023).
[43] T. C. Ralph, Quantum error correction of continuous-variable states against Gaussian noise, Phys. Rev. A **84**, 022339 (2011).
[44] J. Dias and T. C. Ralph, Quantum error correction of continuous-variable states with realistic resources, Phys. Rev. A **97**, 032335 (2018).
[45] S. Slussarenko, M. M. Weston, L. K. Shalm, V. B. Verma, S.-W. Nam, S. Kocsis, T. C. Ralph, and G. J. Pryde, Quantum channel correction outperforming direct transmission, Nat. Commun. **13**, 1 (2022).
[46] S. U. Shringarpure, Y. S. Teo, and H. Jeong, Error suppression in multicomponent cat codes with photon subtraction and teleamplification, ArXiv:2401.04439.
[47] G.-Y. Xiang, T. C. Ralph, A. P. Lund, N. Walk, and G. J. Pryde, Heralded noiseless linear amplification and distillation of entanglement, Nat. Photonics **4**, 316 (2010).
[48] J. Fiurášek, Engineering quantum operations on traveling light beams by multiple photon addition and subtraction, Phys. Rev. A **80**, 053822 (2009).
[49] A. Zavatta, J. Fiurášek, and M. Bellini, A high-fidelity noiseless amplifier for quantum light states, Nat. Photonics **5**, 52 (2011).
[50] F. Ferreyrol, M. Barbieri, R. Blandino, S. Fossier, R. Tualle-Brouri, and P. Grangier, Implementation of a nondeterministic optical noiseless amplifier, Phys. Rev. Lett. **104**, 123603 (2010).
[51] J. Jeffers, Nondeterministic amplifier for two-photon superpositions, Phys. Rev. A **82**, 063828 (2010).
[52] P. Marek and R. Filip, Coherent-state phase concentration by quantum probabilistic amplification, Phys. Rev. A **81**, 022302 (2010).
[53] J. S. Neergaard-Nielsen, Y. Eto, C.-W. Lee, H. Jeong, and M. Sasaki, Quantum tele-amplification with a continuous-variable superposition state, Nat. Photonics **7**, 439 (2013).
[54] J. Zhao, J. Y. Haw, T. Symul, P. K. Lam, and S. M. Assad, Characterization of a measurement-based noiseless linear amplifier and its applications, Phys. Rev. A **96**, 012319 (2017).
[55] S. Zhang and X. Zhang, Photon catalysis acting as noiseless linear amplification and its application in coherence enhancement, Phys. Rev. A **97**, 043830 (2018).
[56] L. Hu, M. Al-amri, Z. Liao, and M. S. Zubairy, Entanglement improvement via a quantum scissor in a realistic environment, Phys. Rev. A **100**, 052322 (2019).
[57] M. He, R. Malaney, and B. A. Burnett, Noiseless linear amplifiers for multimode states, Phys. Rev. A **103**, 012414 (2021).
[58] R. Zhao, J. Guo, and L. Cheng, Entanglement-based single-photon amplification with high fidelity of polarization feature, IEEE Photonics J. **14**, 1 (2022).
[59] M. S. Winnel, N. Hosseinidehaj, and T. C. Ralph, Generalized quantum scissors for noiseless linear amplification, Phys. Rev. A **102**, 063715 (2020).
[60] J. J. Guanzon, M. S. Winnel, A. P. Lund, and T. C. Ralph, Ideal quantum teleamplification up to a selected energy cutoff using linear optics, Phys. Rev. Lett. **128**, 160501 (2022).
[61] J. Fiurášek, Teleportation-based noiseless quantum amplification of coherent states of light, Opt. Express **30**, 1466 (2022).
[62] J. Fiurášek, Optimal linear-optical noiseless quantum amplifiers driven by auxiliary multiphoton Fock states, Phys. Rev. A **105**, 062425 (2022).
[63] W. Zhong, Y.-P. Li, Y.-B. Sheng, and L. Zhou, Quantum scissors for noiseless linear amplification of polarization frequency hyper-encoded coherent state, Europhys. Lett. **140**, 18003 (2022).
[64] J. J. Guanzon, M. S. Winnel, A. P. Lund, and T. C. Ralph, Noiseless linear amplification and loss-tolerant quantum relay using coherent-state superpositions, Phys. Rev. A **108**, 032411 (2023).
[65] A. Z. Goldberg and K. Heshami, Teleamplification on the Borealis boson-sampling device, Phys. Rev. A **108**, 062606 (2023).
[66] C. H. Bennett, G. Brassard, C. Crépeau, R. Jozsa, A. Peres, and W. K. Wootters, Teleporting an unknown quantum state

via dual classical and Einstein-Podolsky-Rosen channels, Phys. Rev. Lett. **70**, 1895 (1993).

[67] D. Su, C. R. Myers, and K. K. Sabapathy, Conversion of Gaussian states to non-Gaussian states using photon-number-resolving detectors, Phys. Rev. A **100**, 052301 (2019).

[68] N. Quesada, L. G. Helt, J. Izaac, J. M. Arrazola, R. Shahrokhshahi, C. R. Myers, and K. K. Sabapathy, Simulating realistic non-Gaussian state preparation, Phys. Rev. A **100**, 022341 (2019).

[69] C. S. Hamilton, R. Kruse, L. Sansoni, S. Barkhofen, C. Silberhorn, and I. Jex, Gaussian boson sampling, Phys. Rev. Lett. **119**, 170501 (2017).

[70] K. K. Sabapathy, H. Qi, J. Izaac, and C. Weedbrook, Production of photonic universal quantum gates enhanced by machine learning, Phys. Rev. A **100**, 012326 (2019).

[71] C. R. Myers, *Investigating photonic quantum computation*, Ph.D. thesis, University of Waterloo, 2007.

[72] J. D. Franson, M. M. Donegan, and B. C. Jacobs, Generation of entangled ancilla states for use in linear optics quantum computing, Phys. Rev. A **69**, 052328 (2004).

[73] A. Hayes, A. Gilchrist, C. Myers, and T. Ralph, Utilizing encoding in scalable linear optics quantum computing, J. Opt. B: Quantum Semiclass. Opt. **6**, 533 (2004).

[74] J. Janszky, P. Domokos, and P. Adam, Coherent states on a circle and quantum interference, Phys. Rev. A **48**, 2213 (1993).

[75] S. Scheel, Permanents in linear optical networks, ArXiv: quant-ph/0406127.

[76] B. T. Gard, K. R. Motes, J. P. Olson, P. P. Rohde, and J. P. Dowling, in *From Atomic to Mesoscale: The Role of Quantum Coherence in Systems of Various Complexities*, edited by S. A. Malinovskaya and I. Novikova (World Scientific Publishing Co, Cambridge, 2015), p. 167.

[77] A. P. Lund, M. J. Bremner, and T. C. Ralph, Quantum sampling problems, boson sampling and quantum supremacy, npj Quantum Inf. **3**, 1 (2017).

[78] W. R. Clements, P. C. Humphreys, B. J. Metcalf, W. S. Kolthammer, and I. A. Walmsley, Optimal design for universal multiport interferometers, Optica **3**, 1460 (2016).

[79] M. S. Winnel, J. J. Guanzon, N. Hosseinidehaj, and T. C. Ralph, Achieving the ultimate end-to-end rates of lossy quantum communication networks, npj Quantum Inf. **8**, 1 (2022).

[80] See https://github.com/JGuanzon/optimal-teleamplifier for our code, which finds the optimal Gaussian-boson-sampling-like device to generate the resource states. This uses the Strawberry Fields PYTHON library, which includes Refs. [81–83].

[81] N. Killoran, J. Izaac, N. Quesada, V. Bergholm, M. Amy, and C. Weedbrook, Strawberry Fields: A software platform for photonic quantum computing, Quantum **3**, 129 (2019).

[82] T. R. Bromley, J. M. Arrazola, S. Jahangiri, J. Izaac, N. Quesada, A. D. Gran, M. Schuld, J. Swinarton, Z. Zabaneh, and N. Killoran, Applications of near-term photonic quantum computers: Software and algorithms, Quantum Sci. Technol. **5**, 034010 (2020).

[83] J. E. Bourassa, N. Quesada, I. Tzitrin, A. Száva, T. Isacsson, J. Izaac, K. K. Sabapathy, G. Dauphinais, and I. Dhand, Fast simulation of bosonic qubits via Gaussian functions in phase space, PRX Quantum **2**, 040315 (2021).